REGULAR ARTICLE

blood advances

Platelet TGF-β1 deficiency decreases liver fibrosis in a mouse model of liver injury

Shahrouz Ghafoory,[1] Rohan Varshney,[1] Tyler Robison,[1] Karim Kouzbari,[1] Sean Woolington,[1] Brennah Murphy,[1] Lijun Xia,[1] and Jasimuddin Ahamed[1,2]

[1]Cardiovascular Biology Research Program, Oklahoma Medical Research Foundation, Oklahoma City, OK; and [2]Department of Biochemistry and Molecular Biology, University of Oklahoma Health Sciences Center, Oklahoma City, OK

Key Points

- Fibrosis in the liver is a common cause of liver disease, partially mediated by platelet TGF-β1 as shown in a mouse model of liver injury.
- Depleting platelet TGF-β1 results in decreased liver fibrosis suggesting that blocking platelet TGF-β1 may ameliorate or prevent fibrosis.

Transforming growth factor-β1 (TGF-β1) signaling in hepatic stellate cells (HSCs) plays a primary role in liver fibrosis, but the source of TGF-β1 is unclear. Because platelets are rich in TGF-β1, we examined the role of platelet TGF-β1 in liver fibrosis by challenging wild-type (WT) mice and mice deficient in platelet TGF-β1 (*PF4CreTgfb1*$^{f/f}$) with carbon tetrachloride (CCl_4), an inducer of acute hepatic injury and chronic fibrosis. CCl_4 elicited equivalent hepatic injury in WT and *PF4CreTgfb1*$^{f/f}$ mice based on loss of cytochrome P450 (*Cyp2e1*) expression, observed at 6 hours and peaking at 3 days after CCl_4 challenge; *PF4CreTgfb1*$^{f/f}$ mice exhibited less liver fibrosis than control mice. Activated platelets were observed during acute liver injury (6 hours), and WT mice with transient platelet depletion (thrombocytopenia) were partially protected from developing fibrosis compared with control mice ($P = .01$), suggesting an association between platelet activation and fibrosis. Transient increases in TGF-β1 levels and Smad2 phosphorylation signaling were observed 6 hours and 3 days, respectively, after CCl_4 challenge in WT, but not *PF4CreTgfb1*$^{f/f}$, mice, suggesting that increased TGF-β1 levels originated from platelet-released TGF-β1 during the initial injury. Numbers of collagen-producing HSCs and myofibroblasts were higher at 3 days and 36 days, respectively, in WT vs *PF4CreTgfb1*$^{f/f}$ mice, suggesting that platelet TGF-β1 may have stimulated HSC transdifferentiation into myofibroblasts. Thus, platelet TGF-β1 partially contributes to liver fibrosis, most likely by initiating profibrotic signaling in HSCs and collagen synthesis. Further studies are required to evaluate whether blocking platelet and TGF-β1 activation during acute liver injury prevents liver fibrosis.

Introduction

Pathologic liver fibrosis, characterized by the accumulation of extracellular matrix protein (mainly collagen), is a frequent consequence of chronic injury and an initiating factor in many liver diseases.[1] Transforming growth factor-β1 (TGF-β1) is a potent profibrotic cytokine that has multifunctional roles in regulating cell proliferation, cell differentiation, wound healing, angiogenesis, and immune function.[2-4] TGF-β1–mediated signaling is a key stimulator of collagen production,[5] and excessive collagen production causes organ fibrosis.[6-8] TGF-β signaling has been shown to contribute to liver fibrosis in both mice and humans.[1,7,9-12] Hepatic stellate cells (HSCs) are the major cell types that can transdifferentiate into collagen-producing myofibroblasts in the liver and lead to pathological fibrosis.[1,11,13,14] TGF-β1 signaling through Smad2 phosphorylation (p-Smad2) is critical for activation

Submitted 24 July 2017; accepted 31 January 2018. DOI 10.1182/bloodadvances.2017010868.

The full-text version of this article contains a data supplement.

of HSCs and their transdifferentiation into myofibroblasts, thus suggesting that this pathway is essential for initiating collagen production and liver fibrosis.[15]

There are several potential sources of TGF-β1 in the liver that may contribute to fibrosis, including HSCs themselves, macrophages, hepatocytes, cholangiocytes, and fibroblasts,[16] but the cellular source(s) of TGF-β1 remain unclear. We previously demonstrated that platelet-derived TGF-β1 contributes to cardiac fibrosis in a high-pressure cardiac overload mouse model[17]; because platelets contain 40 to 100 times more TGF-β1 than other cell types and TGF-β1 is released upon platelet activation,[18-20] we hypothesized that TGF-β1 released from platelets during acute liver injury initiates signaling and thereby induces liver fibrosis. However, the role of platelets in liver fibrosis is controversial because studies have shown both beneficial[21-23] and detrimental[24-27] effects of platelets in liver pathogenesis and fibrosis. Reconciliation of these contradictory findings has not been achieved, nor has the contribution of platelet-derived factors in various conditions been established.

To test our hypothesis, we used a well-established mouse model of carbon tetrachloride (CCl_4)-induced acute and chronic liver injury with fibrosis to compare the effects of CCl_4 in C57BL/6 wild-type (WT) mice and mice carrying a megakaryocyte/platelet-specific targeted conditional deletion of the TGF-β1 gene (*PF4CreTgfb1*$^{f/f}$). We also assessed liver fibrosis in WT mice with acutely induced transient thrombocytopenia caused by a single dose of a platelet-specific anti-glycoprotein 1bα (anti-GP1bα) antibody and compared the results with the fibrosis found in control immunoglobulin G (IgG)-treated mice. Here, we show that TGF-β1 released from platelets during acute liver injury induces profibrotic TGF-β1 signaling, partially causing liver fibrosis. These results suggest a previously unknown role for platelet TGF-β1 in liver fibrosis. Finally, based on our data, we discuss the contradictory roles of platelets in liver fibrosis.

Materials and methods

Mice

C57Bl/6J mice were either obtained from The Jackson Laboratory or bred in-house, and are designated either WT or C57Bl/6 for simplicity. We obtained TGF-β1 allele "floxed" mice (*Tgfb1*$^{flox/flox}$, designated *Tgfb1*$^{f/f}$) from The Jackson Laboratory.[28] We then inbred the *Tgfb1*$^{f/f}$ mice with C57Bl/6 mice for 10 generations to obtain *Tgfb1*$^{f/f}$ on a C57Bl/6 background. These mice were subsequently crossed with transgenic mice expressing Cre recombinase under the control of the megakaryocyte-specific platelet factor 4 (PF4) promoter (*PF4Cre*$^{+/-}$, obtained from The Jackson Laboratory).[29]

To create mice homozygous for both *PF4Cre*$^{+/+}$ and *Tgfb1*$^{f/f}$, we crossed all litters from *PF4Cre*$^{+/+}$*Tgfb1*$^{f/f}$ parents and genotyped these litters until all pups were homozygous for both *PF4Cre*$^{+/+}$ and *Tgfb1*$^{f/f}$, thus suggesting that the parents were homozygous for both alleles. To avoid false positives, we bred the same parents for 3 to 4 rounds; each time, the pups were all homozygous *PF4Cre*$^{+/+}$*Tgfb1*$^{f/f}$, designated *PF4CreTgfb1*$^{f/f}$ for simplicity. We also performed phenotypic characterization by measuring TGF-β1 levels in both platelets and plasma in mice heterozygous and homozygous for *PF4Cre* carrying the *Tgfb1*$^{f/f}$ allele. All mice were housed in a controlled environment (23°C ± 2°C; 12-hour light/dark cycles) and fed a standard diet (PicoLab Rodent Diet). All experimental procedures were approved by the Oklahoma Medical Research Foundation Animal Care and Use Committee. Each mouse was numbered, and all experiments were performed by investigators blinded to the genotype of the mice.

CCl_4-induced liver fibrosis model

Liver fibrosis was induced by a well-established method using CCl_4 in a murine model as previously described.[30] Mice were challenged with an intraperitoneal injection of either 100 μL of mineral oil or CCl_4 (1 μL/g body weight [BW] in a total of 100 μL, prepared by mixing CCl_4 in mineral oil). CCl_4 was injected once, and acute liver injury was monitored after 6 hours, 1 day, and 3 days. To produce chronic injury and fibrosis, CCl_4 was injected repeatedly, as indicated by arrows in Figure 1B. In some cases, mice were injected with antibodies or harvested earlier, at indicated time points.

Tissue preparation and quantification of fibrosis

Detailed methods are presented in the supplemental Methods. Briefly, animals were sacrificed and their livers were fixed in 4% paraformaldehyde and then sectioned. Fibrosis was evaluated histologically by picrosirius red staining. Fibrotic areas were determined by quantifying polarized light images using NIH ImageJ software (supplemental Figure 1B).

Immunohistochemistry

Dual immunohistochemical staining was performed by incubating tissue sections with specific primary antibodies (listed in supplemental Table 1), followed by secondary antibodies tagged with either Alexa 488 or Alexa 594. Fluorescence images were obtained with a Zeiss 710 confocal or Nikon Eclipse 80i fluorescence microscope.

Hydroxyproline assay

Hydroxyproline content in liver tissues was measured according to the manufacturer's instructions using a commercial hydroxyproline assay kit (Sigma-Aldrich).

Statistical analysis

All data are expressed as mean ± standard deviation or standard error of the mean. Statistical calculations were performed using GraphPad Prism, and the Student *t* test was used to determine whether differences were statistically significant. $P < .05$ was considered statistically significant.

Results

Generation of homozygous mice carrying megakaryocyte/platelet-specific deletion of TGF-β1 (PF4CreTgfb1$^{f/f}$)

Mice homozygous for both *PF4Cre*$^{+/+}$ and *Tgfb1*$^{f/f}$ alleles (designated as *PF4CreTgfb1*$^{f/f}$) were generated by crossing heterozygous *PF4Cre*$^{+/-}$ and homozygous *Tgfb1*$^{f/f}$ mice on the C57Bl/6J background for at least 10 generations. Homozygous *PF4CreTgfb1*$^{f/f}$ mice were born in a normal Mendelian ratio and did not display any gross phenotype. They had lower platelet (by ~94%) and plasma (by ~50%) TGF-β1 levels than the WT controls. The TGF-β1 levels in 10^9 platelets per mL were 73.0 ± 10.0 ng in WT mice and 4.0 ± 1.0 ng in *PF4CreTgfb1*$^{f/f}$ mice (Figure 1A; $P < .0001$, n = 7), and in plasma were 2.5 ± 0.7 ng/mL in WT mice and 1.3 ± 0.2 ng/mL in *PF4CreTgfb1*$^{f/f}$ mice ($P < .001$, n = 8).

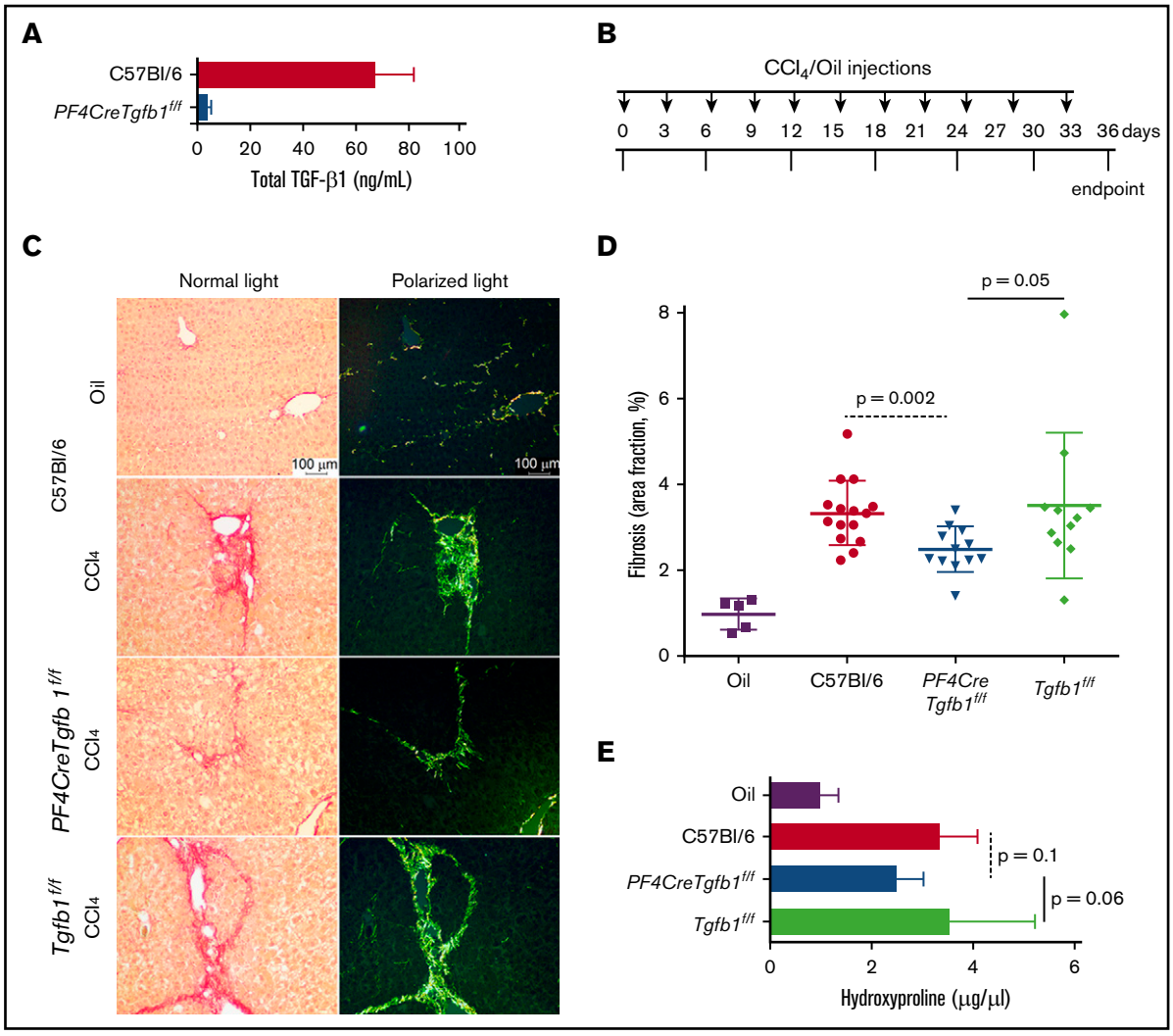

Figure 1. *PF4CreTgfb1*$^{f/f}$ mice are partially protected from developing CCl_4-induced liver fibrosis. (A) Homozygous *PF4CreTgfb1*$^{f/f}$ mice had >90% less TGF-β1 in their platelets than did their littermate controls, as measured with a Duo-Set enzyme-linked immunosorbent assay (ELISA) kit (n = 7; $P < .0001$). (B) Depiction of the experimental protocol showing CCl_4 or oil challenge time points (indicated by arrows) for the duration of the 36-day experiment. (C) Picrosirius red staining was performed on liver sections of oil- or CCl_4-challenged WT or *PF4CreTgfb1*$^{f/f}$ mice according to the protocol shown in panel B. Fibrotic areas in red (images taken under a normal light microscope) and a mixture of green, red, and yellow fluorescent color pictures (taken under polarized light) showed collagen accumulation (representative images are shown). (D) Quantification of fibrotic areas from images taken with a polarized light microscope showed that *PF4CreTgfb1*$^{f/f}$ mice had smaller fibrotic areas than those of C57Bl/6 (WT) or littermate control (*Tgfb1*$^{f/f}$) mice (percentage of picrosirius red–stained fibrosis areas was 2.5% ± 0.5% in *PF4CreTgfb1*$^{f/f}$ mice, 3.3% ± 0.7% in WT mice, 3.5% ± 1.7% in *Tgfb1*$^{f/f}$ mice, and 1.0% ± 0.3% in oil-challenged WT controls; $P = .002$ for *PF4CreTgfb1*$^{f/f}$ mice vs WT mice; $P = .05$ for *PF4CreTgfb1*$^{f/f}$ vs *Tgfb1*$^{f/f}$ mice; $P < .0001$ for CCl_4-challenged vs oil-challenged WT mice). (E) Total collagen content in liver tissue was measured by the hydroxyproline assay, with lower collagen levels found in *PF4CreTgfb1*$^{f/f}$ mice (n = 11) than in WT (n = 9) and *Tgfb1*$^{f/f}$ (n=-5) mice after CCl_4 challenge ($P = .1$ WT vs *PF4CreTgfb1*$^{f/f}$ mice; $P = .06$ *Tgfb1*$^{f/f}$ vs *PF4CreTgfb1*$^{f/f}$ mice).

PF4CreTgfb1$^{f/f}$ mice are partially protected from developing CCl_4-induced liver fibrosis

To study the role of platelet-derived TGF-β1 in liver fibrosis, *PF4CreTgfb1*$^{f/f}$ and WT control mice were challenged with repeated CCl_4 or oil injection as shown in Figure 1B. Two mice (1 in each group) that died before the 36-day experiment end point were excluded from the analysis; there was no difference in death rates between genotypes. Thirty-six days after the initial CCl_4 challenge, liver weight-to-BW ratios were similar in WT and *PF4CreTgfb1*$^{f/f}$ mice, but all WT and *Tgfb1*$^{f/f}$ littermate control mice had severe fibrosis with increased collagen staining (shown in red under normal light and in fluorescent color under polarized light), whereas *PF4CreTgfb1*$^{f/f}$ mice had relatively less fibrosis (Figure 1C). Control WT mice challenged with oil had very little or no fibrosis. Picrosirius red–stained collagen fibers in the fibrotic areas, quantified from whole-liver lobe images taken under polarized light, showed significantly lower levels of fibrosis in *PF4CreTgfb1*$^{f/f}$ mice compared with WT and *Tgfb1*$^{f/f}$ mice at 36 days after the initial CCl_4 challenge (Figure 1D).

The total collagen content in the liver tissue was measured using hydroxyproline assays. Hydroxyproline content was higher after CCl_4 challenge than after oil challenge in WT and *Tgfb1*$^{f/f}$ mice. The mean hydroxyproline content was ~20% lower in *PF4CreTgfb1*$^{f/f}$ mice than in WT and *Tgfb1*$^{f/f}$ mice after CCl_4 challenge (Figure 1E),

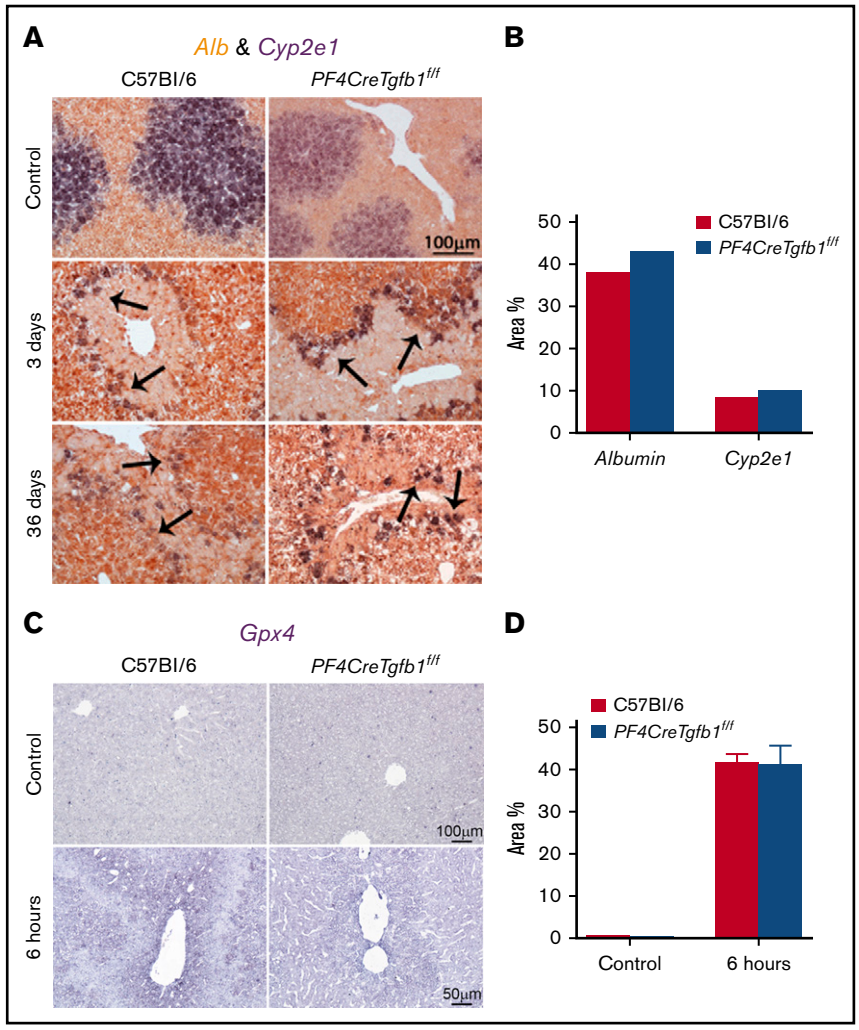

Figure 2. Expression of *Cyp2e1* and *Alb* mRNA in livers after CCl_4 challenge by in situ hybridization. Liver sections were subjected to in situ hybridization with specific probes for *Cyp2e1* and *Alb* genes. (A) Double in situ hybridization showed staining of *Cyp2e1*-expressing cells as a deep blue color stained with NBT/BCIP-substrate bordering the injured areas (indicated by the arrows), mainly in the pericentral vein area. *Alb* expression, shown in deep brown stained with INT/BCIP-substrate, was observed throughout the liver, except in the pericentral vein area, at 3 days and 36 days after CCl_4 challenges in both WT and *PF4CreTgfb1*$^{f/f}$ mice. (B) Quantification of *Cyp2e1* and *Alb* expression showed cells expressing the *Cyp2e1* gene in the injured areas around the pericentral veins in both WT and *PF4CreTgfb1*$^{f/f}$ mice at 3 days after CCl_4 challenge. (C) *Gpx4* expression in the liver was assessed by in situ hybridization using NBT/BCIP-substrate and showed similar expression levels in both WT and *PF4CreTgfb1*$^{f/f}$ mice at 6 hours after CCl_4 challenge. (D) Quantification of *Gpx4* 6 hours after CCl_4 challenge in WT and *PF4CreTgfb1*$^{f/f}$ *mice.*

although the differences were not statistically significant ($P = .1$ vs WT, and $P = .06$ vs *Tgfb1*$^{f/f}$).

CCl_4 challenge induces similar acute liver injury in both PF4CreTgfb1$^{f/f}$ and WT mice

CCl_4 induces liver injury, and the cytochrome P450 isozyme (*Cyp2e1*) is the key metabolic enzyme in the liver that breaks down CCl_4.[30,31] Normally, *Cyp2e1* is primarily expressed in hepatocytes located close to the pericentral veins, whereas albumin (*Alb*) is mostly produced by hepatocytes in the periportal areas; CCl_4 changes the expression patterns of these genes during CCl_4 injury in a time-dependent manner.[31] To evaluate acute liver injury, in situ hybridization was performed before and after CCl_4 challenge, and the expression of *Cyp2e1* and *Alb* genes was evaluated using dual- and single-color in situ hybridization staining. Expression of *Cyp2e1* in the area close to the pericentral vein was uniform in both WT and *PF4CreTgfb1*$^{f/f}$ mice before CCl_4 challenge (Figure 2A; supplemental Figure 2). A time-dependent loss of *Cyp2e1*-expressing cells was observed as early as 6 hours, and maximum loss of these cells was observed 3 days after CCl_4 challenge in both WT and *PF4CreTgfb1*$^{f/f}$ mice (Figure 2A; supplemental Figure 2). *Alb* gene expression was unaffected at all time points (Figure 2A; supplemental Figure 2).

Quantification of both *Cyp2e1*- and *Alb*-expressing cells revealed a similar injury in both *PF4CreTgfb1*$^{f/f}$ and WT mice at 3 days after CCl_4 challenge (Figure 2B). *Cyp2e1*-expressing cells remained on the peripheral borders of the injured areas at 3 days and remained associated with the fibrotic areas bordering the outer layer, whereas *Alb* gene expression was unaffected at 3 days and 36 days after CCl_4 challenge (Figure 2A). These data showed that the first CCl_4 challenge caused maximum injury at 3 days; however, a decrease in injury was observed after subsequent repeated chronic challenges of CCl_4 for 36 days in both genotypes, potentially because of the barrier formed by the *Cyp2e1*-expressing cells along the border of the injured areas, which protected the liver from further injury (Figure 2A; supplemental Figure 2). Quantitative reverse transcription polymerase chain reaction also revealed similar *Alb* and *Cyp2e1* gene expression patterns,[31] with high expression before and loss of expression 3 days after CCl_4 challenge (data not shown). In addition to *Cyp2e1* expression, we also performed hematoxylin-and-eosin and periodic acid–Schiff staining to visualize damaged areas. These areas were nearly equivalent in WT and *PF4CreTgfb1*$^{f/f}$ mice at 6 hours, 1 day, and 3 days, but they were substantially reduced in *PF4CreTgfb1*$^{f/f}$ mice at 36 days compared with WT mice (supplemental Figure 3), consistent with less fibrosis in *PF4CreTgfb1*$^{f/f}$ mice.

To assess the redox environment in the liver during acute injury, in situ hybridization was performed of glutathione peroxidase 4 (*Gpx4*), also known as oxidoreductase, which catalyzes the breakdown of free radicals to glutathione after toxic injury by CCl_4. *Gpx4* messenger RNA (mRNA) expression was upregulated in the injured areas 6 hours after CCl_4 challenge in both WT and *PF4CreTgfb1*$^{f/f}$ mice (Figure 2C-D), thus indicating the occurrence of redox reactions during the initial injury caused by acute CCl_4 challenge. We found a transient increase in lipid peroxidation in the liver 6 hours after CCl_4 challenge in both WT and *PF4CreTgfb1*$^{f/f}$ mice (malondialdehyde assay increased from 0.04 ± 0.002 nM/μL to 0.09 ± 0.02 nM/μL in WT [$P = .02$] and 0.04 ± 0.002 nM/μL to 0.06 ± 0.008 nM/μL in *PF4CreTgfb1*$^{f/f}$ mice [$P = .004$]), indicating *Gpx4* upregulation inducing redox reactions in the damaged area of the liver.

Activated platelets are present in the liver tissue 6 hours after CCl_4 challenge

To investigate whether platelets are activated in the liver after a CCl_4 challenge, cells from liver tissue were isolated and stained with anti-CD41 and Jon/A, an antibody that specifically detects activated platelets, prior to flow cytometry analysis. We observed an increase in CD41 and Jon/A double-positive platelets 6 hours after the CCl_4 challenge compared with untreated liver in WT mice (supplemental Figure 4A). Similarly, platelets double-stained for CD41 and P-selectin, another marker expressed in activated platelets, were also elevated 6 hours after CCl_4 challenge (supplemental Figure 4B), thus indicating their activated state. Activated platelet numbers decreased 1 day after CCl_4 challenge in both WT and *PF4CreTgfb1*$^{f/f}$ liver, indicating transient activation of platelets 6 hours after CCl_4 injection.

Induction of transient thrombocytopenia in WT mice partially protects against CCl_4-induced liver fibrosis

To assess whether transiently decreasing platelets in the circulation after CCl_4 injection would affect liver fibrosis, WT mice were injected with a single dose of platelet-specific monoclonal antibody (mAb) anti-GP1bα (0.25 mg/kg BW) to induce thrombocytopenia 6 hours before the first CCl_4 challenge (Figure 3A). Control mice were injected with an isotype-matched IgG (0.25 mg/kg BW). Pretreatment with anti-GP1bα transiently reduced circulating platelet counts by ~75% compared with mice pretreated with IgG within 1 day after injection (Figure 3B). Platelet counts returned to normal levels within 3 days and were similar at 36 days after 11 CCl_4 injections (Figure 3B). No evidence of hemorrhage or changes in other blood counts were observed during the transient depletion of platelets 1 day after anti-GP1bα injection; however, repeated injections of anti-platelet antibody caused severe bleeding, as expected.[17] Importantly, we found that WT mice pretreated with anti-GP1bα prior to the initial CCl_4 injection displayed less liver fibrosis than those pretreated with IgG (Figure 3C). Quantification of fibrotic areas showed ~30% lower fibrosis in mAb anti-GP1bα–injected animals (n = 7) than in IgG-injected (n = 5) animals ($P = .01$) (Figure 3D). Next, we tested whether transient thrombocytopenia induced at the midpoint of CCl_4 treatment (day 18; supplemental Figure 4C) affected liver fibrosis. We found that a single dose of mAb anti-GP1bα injected 6 hours prior to the seventh of 11 CCl_4 treatments (day 18) also transiently reduced circulating platelet counts (data not shown), but did not decrease fibrosis (supplemental Figure 4D), suggesting that early platelet release of TGF-β1 is particularly important to initiate liver fibrosis.

Plasma levels of total TGF-β1 increase transiently 6 hours after CCl_4 challenge in WT mice but not in PF4CreTgfb1$^{f/f}$ mice

We followed our previously published method of plasma preparation[17] and then measured the levels of total TGF-β1 in plasma, which showed higher total TGF-β1 in WT mice than *PF4CreTgfb1*$^{f/f}$ mice under basal condition. Oil challenge did not affect plasma TGF-β1 levels in either WT or *PF4CreTgfb1*$^{f/f}$ mice. CCl_4 challenge, however, led to a transient increase (of ~20%) in total plasma TGF-β1 at 6 hours in WT mice (2.2 ng/mL before and 3.1 ng/mL after), but no increase in total plasma TGF-β1 in *PF4CreTgfb1*$^{f/f}$ mice (Figure 4A). We also observed higher levels of PF4 and thrombospondin 1 (TSP-1) 6 hours after CCl_4 challenge (data not shown). These data are consistent with transient platelet activation 6 hours after a single CCl_4 challenge.

Active TGF-β1 levels increase transiently in liver tissue 6 hours after CCl_4 challenge in WT mice but not in PF4CreTgfb1$^{f/f}$ mice

To assess whether active TGF-β1 levels increased in liver tissue, the total and active TGF-β1 levels in liver exudates were measured before, 6 hours, 1 day, and 3 days after CCl_4 challenge. Active TGF-β1 levels increased in WT mice but not in *PF4CreTgfb1*$^{f/f}$ mice 6 hours after CCl_4 challenge (Figure 4B). The percentage of active TGF-β1 compared with total TGF-β1 was also increased in WT mice but not in *PF4CreTgfb1*$^{f/f}$ mice (data not shown). These data indicate the occurrence of transient activation of TGF-β1 concomitant with the peak release of total TGF-β1 and platelet activation.

PF4CreTgfb1$^{f/f}$ mice have lower p-Smad2 signaling than WT mice

The consequence of active TGF-β1 generation in liver tissue was also assessed by measuring p-Smad2 as a primary TGF-β1 signaling event during acute injury after CCl_4 challenge. Representative images showed a lower number of p-Smad2$^+$ nuclei in the injured areas in *PF4CreTgfb1*$^{f/f}$ mice than in WT mice (Figure 4C). Quantification of p-Smad2$^+$ nuclei in the injured areas showed ~20% fewer p-Smad2$^+$ nuclei in *PF4CreTgfb1*$^{f/f}$ mice compared with WT mice 3 days after CCl_4 challenge (Figure 4D). Dual staining of p-Smad2$^+$ cells for desmin was also positive, indicating that p-Smad2$^+$ cells are HSCs that are stimulated by platelet-derived TGF-β1 (Figure 4E).

PF4CreTgfb1$^{f/f}$ mice have lower numbers of collagen-expressing activated HSCs and myofibroblasts than WT mice

Because HSCs are the primary cells that transdifferentiate into myofibroblasts and produce collagen during the initial phase of TGF-β1 signaling,[15] in situ hybridization was performed to assess collagen (*Col1a2*) mRNA expression. The results showed a higher number of *Col1a2*-expressing cells in the injured areas of the liver in WT mice than in *PF4CreTgfb1*$^{f/f}$ mice at both 3 days and 36 days after CCl_4 challenge (Figure 5A). To confirm that those *Col1a2*-expressing cells were HSCs, the cells were coimmunostained with desmin and collagen antibodies. A higher number of desmin-positive HSCs (some also positive for collagen) were seen at 3 days in WT mice compared with *PF4CreTgfb1*$^{f/f}$ mice; however, most cells expressed collagen at 36 days and few desmin-positive HSCs were present (Figure 5B),

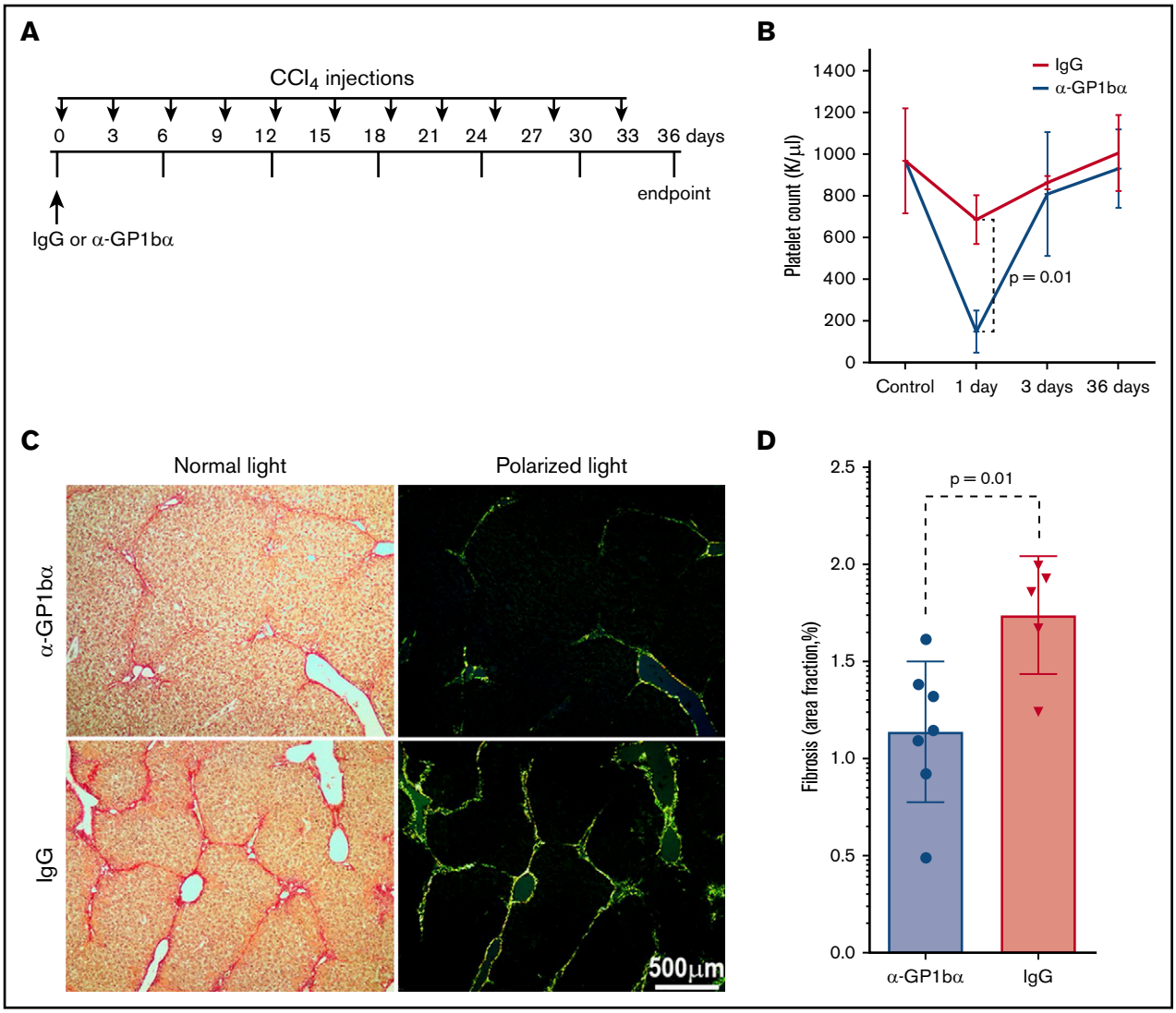

Figure 3. Transient thrombocytopenia partially protects CCl_4-induced liver fibrosis. (A) Experimental protocol showing IgG vs anti-GP-1bα (α-GP1bα) injection times and the CCl_4 challenge time points (indicated by arrows) for the duration of the 36-day experiment. (B) Platelet counts showed marked thrombocytopenia in WT mice 1 day after α-GP1bα antibody administration ($P = .01$ for isotype-matched IgG vs α-GP1bα injections). (C) Picrosirius red staining images at 36 days (both light and polarized light microscopy) showed fibrotic areas in liver sections of WT mice pretreated with IgG or α-GP1bα and then subjected to CCl_4 challenge. (D) Quantification of liver fibrosis showed that mice pretreated with α-GP1bα ($n = 7$) had significantly less fibrosis than those pretreated with IgG ($n = 5$; $P = .01$) at 36 days.

indicating that HSCs were transformed into myofibroblasts. Myofibroblast accumulation is a hallmark of tissue fibrosis, which causes loss of the original markers of the parent cells, gained expression of α–smooth muscle actin (αSMA) and vimentin, and the production of collagen.[32] To confirm whether myofibroblasts were present in the fibrotic areas, liver sections after 36 days of repeated CCl_4 challenge were stained with αSMA and vimentin. Higher numbers of αSMA and vimentin double-positive myofibroblasts were observed in the fibrotic areas of WT mice compared with *PF4CreTgfb1*$^{f/f}$ mice (Figure 5C). The numbers of both αSMA- and vimentin-positive cells were significantly lower in *PF4CreTgfb1*$^{f/f}$ mice than in WT mice (Figure 5D-E).

Discussion

Our finding that *PF4CreTgfb1*$^{f/f}$ mice exhibited significantly less liver fibrosis than WT or littermate control mice after chronic CCl_4 challenge provides evidence that platelet-derived TGF-β1 partially contributes to liver fibrosis in this model. Our new homozygous *PF4CreTgfb1*$^{f/f}$ mice had much lower levels of TGF-β1 in platelets (~94% lower) and in basal plasma (~50% lower) than the levels observed in our previous study using heterozygous *PF4Cre*$^{+/-}$ *Tgfb1*$^{f/f}$ mice, in which TGF-β1 levels were decreased by ~80% in platelets and ~40% in plasma.[17] This difference indicates that introducing 2 alleles of *PF4Cre*$^{+/+}$ recombinase more efficiently depleted TGF-β1 in platelets, resulting in a dramatic reduction in systemic TGF-β1 levels by almost half and confirming our previous finding that platelets contribute significantly to basal plasma levels of TGF-β1.[17]

Our fibrosis quantification methodology is unique and robust because the visible parenchymal fibrosis in the entire lobe of the liver was quantified after exclusion of the visible basal collagen associated with large vessels in the liver (supplemental Figure 1A). Although the

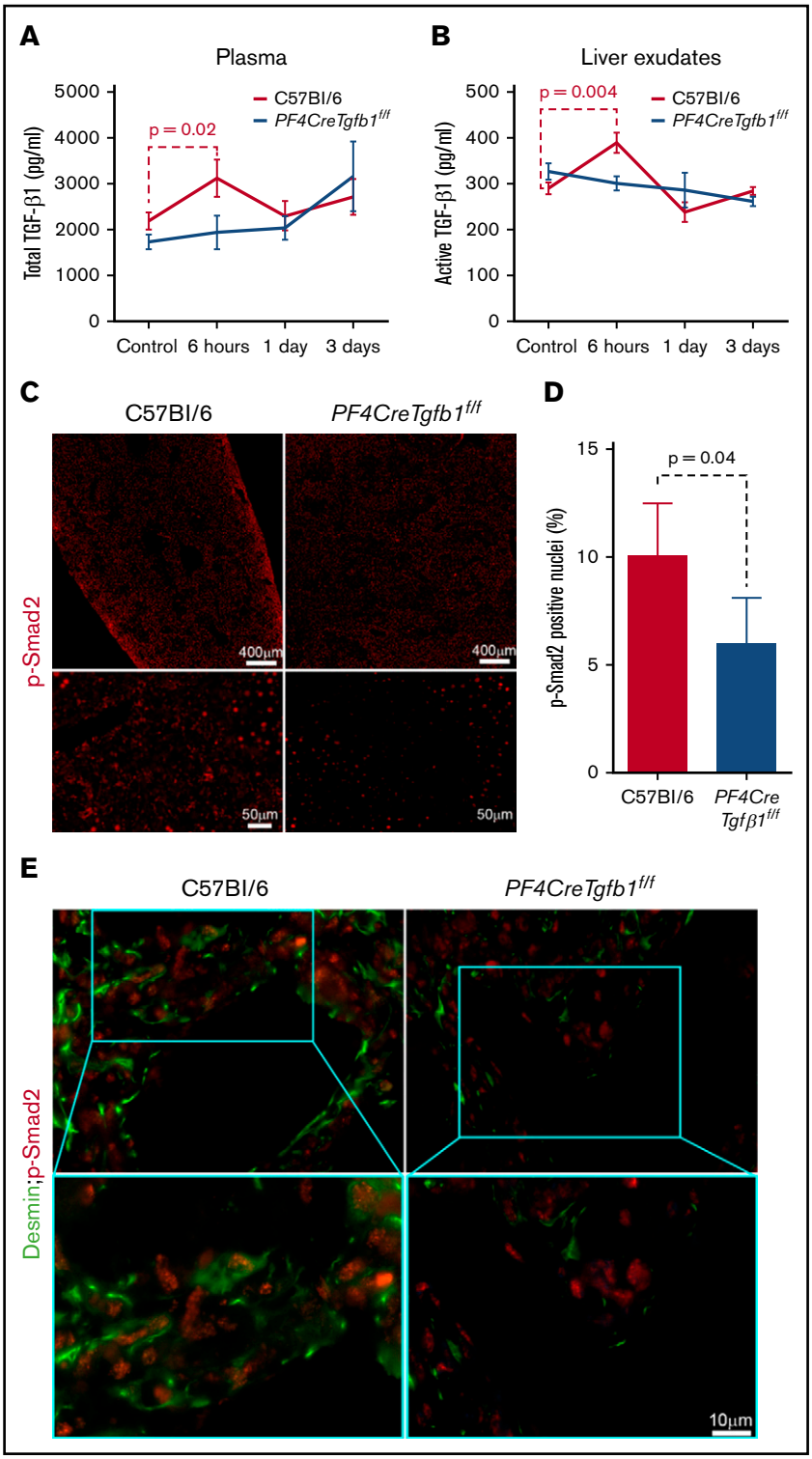

Figure 4. Total and active TGF-β1 and p-Smad2 levels increase transiently after acute CCl_4 challenge in WT mice but not in *PF4CreTgfb1*$^{f/f}$ mice. (A) Total TGF-β1 levels in the plasma of WT and *PF4CreTgfb1*$^{f/f}$ mice at the indicated time points were measured with a modified ELISA protocol using DuoSet kits from R&D Systems. There was a transient increase in the total plasma TGF-β1 in WT mice (n = 7) but not in *PF4CreTgfb1*$^{f/f}$ mice at 6 hours (n = 9). (B) Both active and total TGF-β1 levels in liver exudates were measured by ELISA. Active TGF-β1 levels were higher in WT liver exudates than in *PF4CreTgfb1*$^{f/f}$ liver exudates at 6 hours (n = 5; $P = .004$). (C) p-Smad2 immunostaining showed that most of the phosphorylated signals were in the nuclei (red dots in the tiled pictures of the whole-liver section in the top panels and magnified injured areas in the bottom panels), showing lower levels of p-Smad2 in the injured liver areas of *PF4CreTgfb1*$^{f/f}$ vs WT mice at 3 days after CCl_4 challenge. (D) Quantification of p-Smad2 intensity in the injured areas of the liver sections showed that *PF4CreTgfb1*$^{f/f}$ livers had fewer p-Smad2 cells than did those of WT mice (n = 4; $P = .04$). (E) Sequential dual staining with p-Smad2 and desmin antibodies showed that most of the cells expressing p-Smad2 were desmin-positive HSCs in the injured areas of the liver at 3 days after CCl_4 challenge.

hydroxyproline assay is commonly used to quantify tissue collagen content, it measures both natural basal collagen associated with the basement membrane and blood vessels and pathologic collagen accumulation in fibrosis. Although our visual and quantified data from picrosirius red staining showed a significant difference in liver fibrosis in *PF4CreTgfb1*$^{f/f}$ mice compared with WT and littermate control mice after chronic CCl_4 (Figure 1C-D), our hydroxyproline data from the same groups of mice showed only a decreasing trend (Figure 1E; $P = .1$ and .06). These discrepancies may have been due to some liver sections containing more blood vessels, thus accounting for

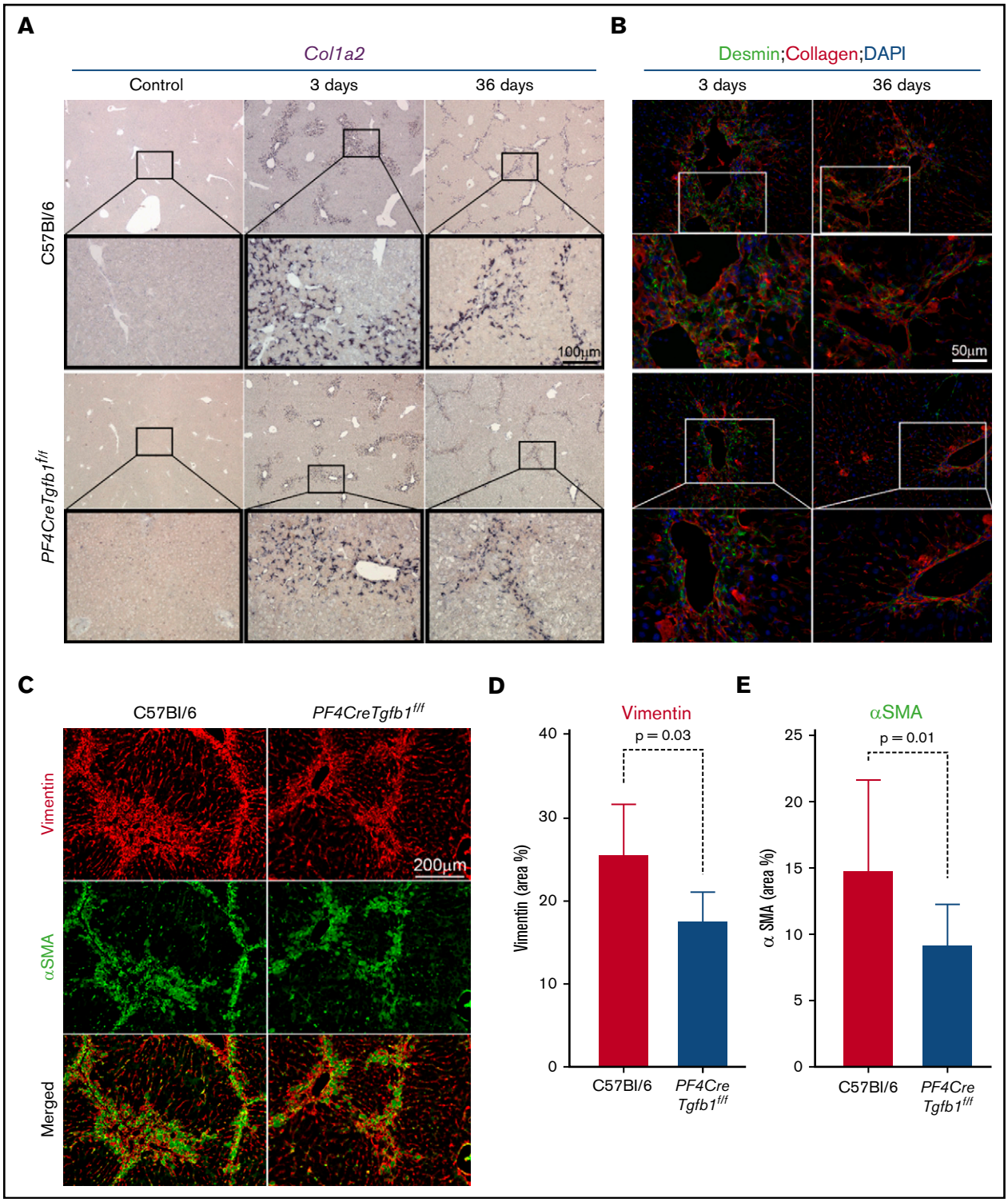

Figure 5. *PF4CreTgfb1*$^{f/f}$ mice have fewer collagen-expressing HSCs and myofibroblasts than WT mice. (A) In situ hybridization of the *Col1a2* probe showed higher collagen-expressing cell accumulation in the injured areas of the liver in WT vs *PF4CreTgfb1*$^{f/f}$ mice at 3 days and 36 days after CCl_4 challenge. Higher-magnification images (boxed) showed that the morphology of those cells resembled HSCs. (B) To confirm that they were HSCs, liver sections were costained with anti-desmin and collagen antibodies; double-positive cells started to appear at 3 days and in the fibrotic areas at 36 days after CCl_4 challenge. (C) Dual staining with myofibroblast markers αSMA (green) and vimentin (red) showed double-positive (yellow) cells at 36 days after CCl_4 challenge in the WT and *PF4CreTgfb1*$^{f/f}$ mice. Quantification of vimentin- (D) and αSMA- (E) positive cells in *PF4CreTgfb1*$^{f/f}$ (n = 7) vs WT (n = 12) mice. DAPI, 4′,6-diamidino-2-phenylindole.

basal collagen, which may be a confounding factor in quantifying collagen accumulation in pathologic fibrotic phenotypes. Therefore, our visual image processing, including carefully removing blood vessels, and computational quantification data for fibrosis are much more reliable. Our in situ hybridization results showing expression of *Cyp2e1* (which changes upon CCl_4 challenge) and *Alb* genes indicated that WT and *PF4CreTgfb1*$^{f/f}$ mice sustained equivalent acute liver injury induced by CCl_4 challenge, thus suggesting that the lower amount of fibrosis observed in *PF4CreTgfb1*$^{f/f}$ mice may not be due to less severe initial injury caused by CCl_4 but instead may be the result of platelet-derived TGF-β1–mediated profibrotic signaling.

Sterile inflammation (SI) is a key process in drug- or toxin-induced liver injury in the absence of pathogens,[33] and SI-driven liver diseases are common in industrially developed countries; unfortunately, there is no specific treatment of fibrosis. We used the CCl_4-induced liver fibrosis model because it simulates SI-induced pathology and is a reproducible model,[34] whereas the commonly used bile-duct ligation model requires surgery and can often be associated with mortality and platelet activation associated with surgery.[35] Although our model involves an artificial and aggressive liver injury, other natural chronic liver injury models should be tested in the future to assess the role of platelet-derived TGF-β1 in models of alcohol-induced, acetaminophen overdose–induced, and viral or parasite infection–induced liver fibrosis.[34]

Recently, Ito et al have shown that platelets can pass through toxin-induced injured liver sinusoidal endothelial layers.[36] These data are consistent with our finding that platelets in injured areas were activated, which is unsurprising given that platelets are activated after contact with extracellular matrix.[37] However, the timing of initial transient platelet activation is interesting because it correlated with transient increases in total TGF-β1 in both plasma and liver tissue 6 hours after the first CCl_4 challenge, indicating that the release of TGF-β1 from platelets occurs in acute liver injury as early as 6 hours after CCl_4 challenge.

Our experiments with transient platelet depletion before injury using mAb anti-GP1bα are protective, indicating that initial platelet activation is important, although the possibility of later contributions of platelets in the process cannot be excluded. More importantly, the detection of active TGF-β1 in liver exudates in the basal condition supports the importance of TGF-β1 signaling in liver homeostasis,[16] but the transient spike in TGF-β1 activity in WT mice and increased p-Smad2$^+$ cells during the initial liver injury suggests that platelet-derived TGF-β1 release and subsequent activation most likely initiates profibrogenic signaling that may lead to liver fibrosis. However, further time-course and systematic analyses using lineage-tracing experiments are required to determine the mechanism by which platelet TGF-β1 initiates signaling that leads to activation of cellular transformation, which ultimately results in liver fibrosis.

A redox environment during liver injury can be assumed, as supported by our data that upregulation of *Gpx4*, an oxidoreductase enzyme capable of catalyzing oxidation, activates TGF-β1.[38] A high-redox environment generates reactive oxygen species, which also activate latent TGF-β1.[8,39] Other possible mechanisms of TGF-β1 activation in the liver may include changes in shear force; previously, we have shown that shear can activate latent TGF-β1.[18] It has been demonstrated that during liver injury, sinusoidal endothelial cells sense changes in shear stress,[40] but measuring shear stress change and correlating this change with active TGF-β1 is challenging in vivo.[41] Moreover, our group and others have shown that TSP-1 activates TGF-β1,[42,43] and a recent review has summarized the role of TSP-1 in liver fibrosis.[44] Therefore, TSP-1–mediated TGF-β1 activation under shear stress change may also be a potential mechanism of TGF-β1 activation in the liver. Moreover, protease-degraded fragments of latency-associated protein/TGF-β1 have been detected using specific epitope-recognizing antibodies in patients and animals with liver fibrosis, thus suggesting that protease-mediated TGF-β1 activation occurs during liver fibrosis, which can be detected in plasma.[45] Further experiments are required to identify the mechanism(s) of TGF-β1 activation in the liver.

TGF-β1 signaling is a strong stimulator of HSC transdifferentiation into collagen-producing myofibroblasts,[15] the primary cell type involved in pathologic liver fibrosis.[46-48] Our findings showed that mice deficient in platelet TGF-β1 (*PF4CreTgfb1*$^{f/f}$) have less p-Smad2 signaling in the injured areas, lower expression of *Col1a2* genes in HSCs, fewer collagen-producing myofibroblasts, and less fibrosis in the liver, as compared with WT mice, thus suggesting that platelet TGF-β1 may have direct and/or indirect effects on HSCs. However, the possible effects of platelet TGF-β1 on other cell types in the liver, including portal fibroblasts, macrophages, hepatocytes, endothelial cells, and stem cells, cannot be eliminated in the pathogenesis of liver fibrosis.[49] Indeed, both in vitro and in vivo evidence have shown that sinusoidal endothelial cells and hepatocytes can internalize platelets,[41,50] thereby indicating that direct contact of platelets with other liver cells is possible during injury. Moreover, a recent study showed that liver macrophages activated platelets via a receptor that requires glycosylation,[51] suggesting a possible role of liver macrophages in regulating liver fibrosis. Because platelet TGF-β1 does not account for all of the induction of liver fibrosis, the possibility that other cellular sources of TGF-β1 might influence liver fibrosis remains to be determined. Future studies with conditional deletion of TGF-β1 in other liver cells, along with inflammatory cell depletion and pharmacological inhibitor experiments, are required to address these issues.

The role of platelets in liver fibrosis is controversial, with some studies showing a beneficial role of platelets on liver function,[21-23] as suggested by a clinical trial indicating that increased platelet numbers induced by platelet transfusion improve liver function in patients with chronic liver disease,[52] whereas other studies have shown detrimental effects.[24-27] These conflicting findings could suggest a dual role of platelets that may be explained by their differential activation status and potential ability to release various factors. As shown by Italiano et al, platelets contain both antiangiogenic and proangiogenic factors that are differentially released after platelet activation by stimulation of various receptors,[53] in agreement with the concept that platelets play a dual role in regulating angiogenesis. A similar scenario may occur in terms of platelets regulating fibrosis vs liver regeneration, by releasing factors that cause fibrosis, such as TGF-β1, or factors that mobilize and promote proliferation of stem cells and progenitor cells during regeneration, such as serotonin or stromal-cell derived factor-1. A recent study reported that reprogramming myofibroblasts and stimulating stem cells differentially regulates liver fibrosis and regeneration in a manner dependent on transcriptional expression and the duration of TGF-β1 stimulation,[54,55] thus supporting the dual-role concept of platelets, which might

be differentially mediated by platelet-derived TGF-β1. Further studies with genetically modified mouse models, including lineage-tracing experiments, are required to resolve these complicated issues.

This study provides new insights into the mechanism by which platelet-derived TGF-β1 may induce liver fibrosis. Our findings suggest that future studies blocking activation of platelets and/or TGF-β1 may lead to new therapeutic approaches to prevent hepatic fibrosis.

Acknowledgments

The authors thank the members of the Cardiovascular Biology Research Program at Oklahoma Medical Research Foundation for their kind assistance in allowing the use of their instruments. The authors also thank Melinda West for mouse colony maintenance and M. K. Occhipinti and A. Anderson (life science editors) for editorial assistance.

This work was supported in part by the National Institutes of Health, National Heart, Lung, and Blood Institute (grant HL123605) (J.A.), National Institute of General Medical Sciences (grant GM114731), and National Cancer Institute (grant CA213987).

Authorship

Contribution: S.G. performed the experiments, interpreted the data, created figures, and assisted in drafting the manuscript; R.V. and T.R. assisted with and performed some experiments and provided valuable suggestions; B.M., K.K., and S.W. performed some experiments; L.X. provided intellectual feedback and valuable comments; and J.A. conceived the idea, provided intellectual feedback, supervised the project, and drafted the manuscript.

Conflict-of-interest disclosure: The authors declare no competing financial interests.

ORCID profile: J.A., 0000-0001-6455-0296.

Correspondence: Jasimuddin Ahamed, Cardiovascular Biology Research Program, Oklahoma Medical Research Foundation, 825 NE 13th St, Oklahoma City, OK 73104; e-mail: ahamedj@omrf.org.

References

1. Bataller R, Brenner DA. Liver fibrosis. *J Clin Invest*. 2005;115(2):209-218.
2. Massagué J. The transforming growth factor-beta family. *Annu Rev Cell Biol*. 1990;6(1):597-641.
3. Mishra L, Derynck R, Mishra B. Transforming growth factor-beta signaling in stem cells and cancer. *Science*. 2005;310(5745):68-71.
4. Rahimi RA, Leof EB. TGF-beta signaling: a tale of two responses. *J Cell Biochem*. 2007;102(3):593-608.
5. Bauer M, Schuppan D. TGFbeta1 in liver fibrosis: time to change paradigms? *FEBS Lett*. 2001;502(1-2):1-3.
6. Blobe GC, Schiemann WP, Lodish HF. Role of transforming growth factor beta in human disease. *N Engl J Med*. 2000;342(18):1350-1358.
7. Border WA, Noble NA. Transforming growth factor beta in tissue fibrosis. *N Engl J Med*. 1994;331(19):1286-1292.
8. Ahamed J, Laurence J. Role of platelet-derived transforming growth factor-β1 and reactive oxygen species in radiation-induced organ fibrosis. *Antioxid Redox Signal*. 2017;27(13):977-988.
9. Dooley S, ten Dijke P. TGF-β in progression of liver disease. *Cell Tissue Res*. 2012;347(1):245-256.
10. Gressner AM, Weiskirchen R, Breitkopf K, Dooley S. Roles of TGF-beta in hepatic fibrosis. *Front Biosci*. 2002;7(4):d793-d807.
11. Seki E, De Minicis S, Osterreicher CH, et al. TLR4 enhances TGF-beta signaling and hepatic fibrosis. *Nat Med*. 2007;13(11):1324-1332.
12. Trautwein C, Friedman SL, Schuppan D, Pinzani M. Hepatic fibrosis: concept to treatment. *J Hepatol*. 2015;62(suppl 1):S15-S24.
13. Friedman SL. Hepatic stellate cells: protean, multifunctional, and enigmatic cells of the liver. *Physiol Rev*. 2008;88(1):125-172.
14. Mederacke I, Hsu CC, Troeger JS, et al. Fate tracing reveals hepatic stellate cells as dominant contributors to liver fibrosis independent of its aetiology. *Nat Commun*. 2013;4:2823.
15. Dooley S, Delvoux B, Streckert M, et al. Transforming growth factor beta signal transduction in hepatic stellate cells via Smad2/3 phosphorylation, a pathway that is abrogated during in vitro progression to myofibroblasts. TGFbeta signal transduction during transdifferentiation of hepatic stellate cells. *FEBS Lett*. 2001;502(1-2):4-10.
16. Schon HT, Weiskirchen R. Immunomodulatory effects of transforming growth factor-β in the liver. *Hepatobiliary Surg Nutr*. 2014;3(6):386-406.
17. Meyer A, Wang W, Qu J, et al. Platelet TGF-β1 contributions to plasma TGF-β1, cardiac fibrosis, and systolic dysfunction in a mouse model of pressure overload. *Blood*. 2012;119(4):1064-1074.
18. Ahamed J, Burg N, Yoshinaga K, Janczak CA, Rifkin DB, Coller BS. In vitro and in vivo evidence for shear-induced activation of latent transforming growth factor-beta1. *Blood*. 2008;112(9):3650-3660.
19. Assoian RK, Komoriya A, Meyers CA, Miller DM, Sporn MB. Transforming growth factor-beta in human platelets. Identification of a major storage site, purification, and characterization. *J Biol Chem*. 1983;258(11):7155-7160.
20. Ahamed J, Terry H, Choi ME, Laurence J. Transforming growth factor-β1-mediated cardiac fibrosis: potential role in HIV and HIV/antiretroviral therapy-linked cardiovascular disease. *AIDS*. 2016;30(4):535-542.
21. Kodama T, Takehara T, Hikita H, et al. Thrombocytopenia exacerbates cholestasis-induced liver fibrosis in mice. *Gastroenterology*. 2010;138(7):2487-2498.
22. Takahashi K, Murata S, Fukunaga K, Ohkohchi N. Human platelets inhibit liver fibrosis in severe combined immunodeficiency mice. *World J Gastroenterol*. 2013;19(32):5250-5260.

23. Watanabe M, Murata S, Hashimoto I, et al. Platelets contribute to the reduction of liver fibrosis in mice. *J Gastroenterol Hepatol*. 2009; 24(1):78-89.
24. Celikbilek M. Letter: increased platelet activation in chronic liver disease–hit two targets with a single shot. *Aliment Pharmacol Ther*. 2016;43(9):1023.
25. Fujita K, Nozaki Y, Wada K, et al. Effectiveness of antiplatelet drugs against experimental non-alcoholic fatty liver disease. *Gut*. 2008;57(11):1583-1591.
26. Lang PA, Contaldo C, Georgiev P, et al. Aggravation of viral hepatitis by platelet-derived serotonin. *Nat Med*. 2008;14(7):756-761.
27. Sitia G, Aiolfi R, Di Lucia P, et al. Antiplatelet therapy prevents hepatocellular carcinoma and improves survival in a mouse model of chronic hepatitis B. *Proc Natl Acad Sci USA*. 2012;109(32):E2165-E2172.
28. Azhar M, Yin M, Bommireddy R, et al. Generation of mice with a conditional allele for transforming growth factor beta 1 gene. *Genesis*. 2009;47(6):423-431.
29. Tiedt R, Schomber T, Hao-Shen H, Skoda RC. Pf4-Cre transgenic mice allow the generation of lineage-restricted gene knockouts for studying megakaryocyte and platelet function in vivo. *Blood*. 2007;109(4):1503-1506.
30. Recknagel RO, Glende EA Jr, Dolak JA, Waller RL. Mechanisms of carbon tetrachloride toxicity. *Pharmacol Ther*. 1989;43(1):139-154.
31. Ghafoory S, Breitkopf-Heinlein K, Li Q, Scholl C, Dooley S, Wölfl S. Zonation of nitrogen and glucose metabolism gene expression upon acute liver damage in mouse. *PLoS One*. 2013;8(10):e78262.
32. Watsky MA, Weber KT, Sun Y, Postlethwaite A. New insights into the mechanism of fibroblast to myofibroblast transformation and associated pathologies. *Int Rev Cell Mol Biol*. 2010;282:165-192.
33. Kubes P, Mehal WZ. Sterile inflammation in the liver. *Gastroenterology*. 2012;143(5):1158-1172.
34. Hayashi H, Sakai T. Animal models for the study of liver fibrosis: new insights from knockout mouse models. *Am J Physiol Gastrointest Liver Physiol*. 2011;300(5):G729-G738.
35. Tag CG, Sauer-Lehnen S, Weiskirchen S, et al. Bile duct ligation in mice: induction of inflammatory liver injury and fibrosis by obstructive cholestasis. *J Vis Exp*. 2015;(96).
36. Ito Y, Abril ER, Bethea NW, et al. Mechanisms and pathophysiological implications of sinusoidal endothelial cell gap formation following treatment with galactosamine/endotoxin in mice. *Am J Physiol Gastrointest Liver Physiol*. 2006;291(2):G211-G218.
37. Bergmeier W, Hynes RO. Extracellular matrix proteins in hemostasis and thrombosis. *Cold Spring Harb Perspect Biol*. 2012;4(2):a005132.
38. Brophy TM, Coller BS, Ahamed J. Identification of the thiol isomerase-binding peptide, mastoparan, as a novel inhibitor of shear-induced transforming growth factor β1 (TGF-β1) activation. *J Biol Chem*. 2013;288(15):10628-10639.
39. Barcellos-Hoff MH, Dix TA. Redox-mediated activation of latent transforming growth factor-beta 1. *Mol Endocrinol*. 1996;10(9): 1077-1083.
40. Braet F, Shleper M, Paizi M, et al. Liver sinusoidal endothelial cell modulation upon resection and shear stress in vitro. *Comp Hepatol*. 2004;3(1):7.
41. Poisson J, Lemoinne S, Boulanger C, et al. Liver sinusoidal endothelial cells: Physiology and role in liver diseases. *J Hepatol*. 2017; 66(1):212-227.
42. Ahamed J, Janczak CA, Wittkowski KM, Coller BS. In vitro and in vivo evidence that thrombospondin-1 (TSP-1) contributes to stirring- and shear-dependent activation of platelet-derived TGF-beta1. *PLoS One*. 2009;4(8):e6608.
43. Ribeiro SM, Poczatek M, Schultz-Cherry S, Villain M, Murphy-Ullrich JE. The activation sequence of thrombospondin-1 interacts with the latency-associated peptide to regulate activation of latent transforming growth factor-beta. *J Biol Chem*. 1999;274(19):13586-13593.
44. Li Y, Turpin CP, Wang S. Role of thrombospondin 1 in liver diseases. *Hepatol Res*. 2017;47(2):186-193.
45. Hara M, Kirita A, Kondo W, et al. LAP degradation product reflects plasma kallikrein-dependent TGF-β activation in patients with hepatic fibrosis. *Springerplus*. 2014;3(1):221.
46. Friedman SL. Mechanisms of hepatic fibrogenesis. *Gastroenterology*. 2008;134(6):1655-1669.
47. Kalluri R, Weinberg RA. The basics of epithelial-mesenchymal transition. *J Clin Invest*. 2009;119(6):1420-1428.
48. Lee UE, Friedman SL. Mechanisms of hepatic fibrogenesis. *Best Pract Res Clin Gastroenterol*. 2011;25(2):195-206.
49. Iwaisako K, Jiang C, Zhang M, et al. Origin of myofibroblasts in the fibrotic liver in mice. *Proc Natl Acad Sci USA*. 2014;111(32):E3297-E3305.
50. Li J, van der Wal DE, Zhu G, et al. Desialylation is a mechanism of Fc-independent platelet clearance and a therapeutic target in immune thrombocytopenia. *Nat Commun*. 2015;6(1):7737.
51. Li Y, Fu J, Ling Y, et al. Sialylation on O-glycans protects platelets from clearance by liver Kupffer cells. *Proc Natl Acad Sci USA*. 2017;114(31): 8360-8365.
52. Kurokawa T, Zheng YW, Ohkohchi N. Novel functions of platelets in the liver. *J Gastroenterol Hepatol*. 2016;31(4):745-751.
53. Italiano JE Jr, Richardson JL, Patel-Hett S, et al. Angiogenesis is regulated by a novel mechanism: pro- and antiangiogenic proteins are organized into separate platelet alpha granules and differentially released. *Blood*. 2008;111(3):1227-1233.
54. Rezvani M, Español-Suñer R, Malato Y, et al. In vivo hepatic reprogramming of myofibroblasts with AAV vectors as a therapeutic strategy for liver fibrosis. *Cell Stem Cell*. 2016;18(6):809-816.
55. Yang AT, Hu DD, Wang P, et al. TGF-beta1 induces the dual regulation of hepatic progenitor cells with both anti- and proliver fibrosis. *Stem Cells Int*. 2016;2016:1492694.